$BaTi(O_{1-x}S_x)_3$ chalcogenide perovskite thin films with band gap ideal for solar cell applications

F. L. González-Gregorio[a], R. Gómez-Rosales[a], A. I. Nuñéz-Oliva[a], P. Y. Rosales-Medina[a], E. de la O-Cuevas[b], J. A. Vargas-Téllez[a], H. Tototzintle-Huitle[a], and J. J. Ortega[a]

[a]*Unidad Académica de Física, Universidad Autónoma de Zacatecas, Calzada Solidaridad esq. Paseo de la Bufa, Fracc. Progreso, 98060, Zacatecas, México.*
[b]*Unidad Académica de Biologia, Universidad Autónoma de Zacatecas, Preparatoria, Hidraulica, Zacatecas, 98068, Zacatecas, México.*

Received 15 December 2025; accepted 18 March 2026

$BaTi(O_{1-x}S_x)_3$ chalcogenide perovskite thin films were deposited by the spin coating technique, using a solution formed by a powder of $BaTi(O_{0.5}S_{0.5})_3$ perovskite compound previously synthesized and ethanol as a solvent. To obtain the powdered $BaTi(O_{1-x}S_x)_3$ perovskite compound used as precursor material, a sulfidization process to barium titanate ($BaTiO_3$) was carried out in a constant flow CS_2/Ar atmosphere at a temperature of 600°C for four hours. After depositing, the films were annealed for one hour in a tube furnace at a temperature of 400°C, in an Ar and CS_2 reactive atmosphere. EDX-RF, XRD, FTIR and Uv-Vis-NIR techniques were used to analyze the structural, vibrational, and optical properties of the films. All deposited and annealed films showed the hexagonal crystalline structure typical of $BaTiS_3$ perovskite with an absorption coefficient greater than 4×10^4 cm^{-1} in the range 600 to 950 nm. The band gap of the $BaTi(O_{1-x}S_x)_3$ chalcogenide perovskite thin films was narrowed as a function of the concentration of sulfur in the sample. The final band gap values obtained were 1.51, 1.45 and 1.35 eV for sulfur percentages of 24.3, 25.3 and 28.7, respectively. These results suggest that $BaTi(O_{1-x}S_x)_3$ chalcogenide perovskites have an ideal band gap for potential applications in perovskite solar cells.

Keywords: Chalcogenide perovskite; oxisulfide perovskite; $BaTi(OS)_3$; band gap engineering; perovskite thin films.

DOI: https://doi.org/10.31349/RevMexFis.72.041601

1. Introduction

In the last seven years, chalcogenide perovskites (perovskites with oxygen, sulfur, or selenium as anions) have been proposed as promising alternatives for photovoltaic applications [1–3] to replace organometallic halide perovskites, which, as is well known, have several problems of phase stability when exposed to the environment. In addition to the innate toxicity represented by the use of lead [4, 5]. Mostly recent theoretical reports, which are based on numerical calculations and density functional theories (DFT), have predicted properties for a large number of chalcogenide perovskites, desirable structural and optical properties for photovoltaic applications, such as a high degree of thermodynamic and atmospheric stability, strong absorption in the spectrum of solar radiation, direct and allowed band gap, and tunable band gap in the ultraviolet, visible and near-infrared region, among others [6–10].

It is well known that the band gap of semiconductors in photovoltaic device applications should be within the range of 1.1 to 1.4 eV, according to the Shockley Quessier limit [11, 12]. In the case of perovskites solar cells, the most efficient solar cells use perovskites with a band gap in the range of 1.3 to 1.6 eV [13]. Although chalcogenide perovskites report tunable band gaps from 2.5 to less than 0.5 eV, so far there have been no experimental reports of the synthesis of chalcogenide perovskites with a band gap between 1.4 and 1.3 eV. In the last five years, several experimental studies have been conducted on the synthesis of $BaZrS_3$, $Ba(Ti_{1-x}Zr_x)S_3$ and $BaZr(S_{1-x}Se_x)_3$ perovskites [12–15]. However, currently, the average values of the experimental results report values of 1.9 eV for $BaZrS_3$ [14], while for $Ba(Ti_{1-x}Zr_x)S_3$ it is reported that it can be reduced to 1.6 eV, which limits its application as an active layer in perovskite solar cells.

For these reasons, theoretical and experimental studies have recently begun on the chalcogenide $BaTiS_3$, which have shown excellent optoelectronic properties [16] and thus could be used in photodetectors, solar cells, etc. The predominant synthesis of this compound is carried out by chemical vapor transport (CVT) at temperatures above 900°C [16, 17], and this material has also been synthesized using microcrystalline reconstruction and pulsed laser methods [18, 19]. However, currently the methods for depositing $BaTIS_3$ thin films are very scarce, since they require extremely high temperatures; therefore, the fabrication of thin films by both physical and chemical methods is quite limited. Another obstacle to using this material as an active layer in solar cells is the size of the bandgap, which lies in a range from 0.27 to 0.9 eV [20].

Despite the same objective, a new theoretical proposal was presented to engineer the band gap of $BaTiS_3$ replacing sulfur with oxygen [21–24], and recently, an experimental report confirmed that it is effectively possible to take control of the band gap through the percentage of sulfur and oxygen in the $BaTi(O_{1-x}S_x)_3$ powder [25]. These results completely opened a new investigation line for experimental investigation of the fundamental properties of $BaTi(O_{1-x}S_x)_3$ thin

films because it is well known that many times the properties of a bulk material could change completely when it is deposited in a thin film. Therefore, the deposition of thin films of chalcogenide perovskite has been an experimental challenge.

As already mentioned, there is limited information to date on the use of the chalcogenide perovskite compound $BaTi(O_{1-x}S_x)_3$ as an active layer in solar cell structures. Based on the results obtained and presented in this work, we assess the feasibility of using this material as an active layer in solar cells. Furthermore, we propose, as future work, the fabrication of a p-i-n type structure, employing spiro-MeOTAD as the p-type conductor, the perovskite compound as the intrinsic layer, and TiO_2 as the n-type semiconductor.

This article presents a study of the deposition and the structural and optical properties of $BaTi(O_{1-x}S_x)_3$ chalcogenide perovskite thin films. These films were deposited using the spin-coating technique, which is simple and highly reproducible, and after deposition, an annealing treatment was carried out at the relatively low temperature of 400°C in a reactive Ar/CS_2 atmosphere. A complete analysis of the crystalline structure of $BaTi(O_{1-x}S_x)_3$ is presented, as well as its optical and vibrational properties and the correlation between them. Moreover, the results obtained confirm that these chalcogenide perovskite thin films present the requested high absorption coefficient, and a band gap very close to the ideal for the S-Q limit, which can be reduced as a function of sulfur concentration, corroborating in an experimental way the properties reported in recent articles.

2. Experimental details

Thin films of $BaTi(O_{1-x}S_x)_3$ perovskite compounds were deposited using the spin coating technique, for these deposits, a solution made up of the perovskite compound $BaTi(O_{0.5}S_{0.5})_3$ and ethanol as solvent was used, and the molar concentration of the solution was 0.5 (128.65 g/L), this solution was mixed in an ultrasonic bath for 30 minutes. To obtain the powdered $BaTi(O_{1-x}S_x)_3$ perovskite compound used as precursor material, a sulfidization process to barium titanate ($BaTiO_3$) was carried out in a constant flow CS_2/Ar atmosphere at a temperature of 600°C for four hours. All deposits were made at a constant rotation speed of 780 rpm on glass substrates, the amount of solution used in each deposit varied, these amounts were 1, 2, and 3 drops, each drop of approximately 50 μL. After depositing, all films were heat treated in a quartz tubular furnace at 400 Â°C, in an atmosphere of Ar and CS_2 with a flow rate of 1 lpm, for one hour.

The elemental composition and thickness of the films were measured using a Rigaku EDX-RF spectrometer NEX QC+ Quantez model. The crystalline structure present in the perovskite films was obtained with Bruker D8 ADVANCED ECO equipment and the diffraction of the films was carried out at room temperature, using Cu K_α radiation and a wavelength of 1.54056 Å at a 2θ angle. The absorption spectra were obtained with the Ocean Optics USB4000 Fiber Optic Spectrometer.

3. Results

3.1. Structural properties

3.1.1. Elemental composition

The elemental composition and thickness of the thin films of perovskite compounds $BaTi(O_{1-x}S_x)_3$ were obtained by the energy-dispersive X-ray fluorescence spectroscopy technique. The stoichiometry of the thin films was obtained using the percentages of mass measured for each element present in the samples and the thicknesses of each film were estimated by the NEXT software included as a package of Rigaku EDX-RF spectrometer. The estimated thicknesses of the films were 289, 514, and 943 nm, corresponding to the films deposited by 1, 2, and 3 drops, respectively.

As deposited, the films conserved the same stoichiometry of the $BaTi(O_{0.5}S_{0.5})_3$ precursor powder, independently of the thickness of the sample. However, after reactive annealing treatment, the films showed an increase in sulfur concentration at the same time that oxygen concentration decreased, compared to the precursor perovskite compound used to deposit the films. In all cases, an inverse relationship was observed between the thickness of the films and the increase in sulfur in them, that is, at a lower thickness, a greater amount of sulfur in the films. The percentage in mass of sulfur increased from 16.6 present in the solution deposited to 24.3, 25.3, and 28.7 in films with thicknesses of 943, 514, and 289 nm, respectively. From these data, the stoichiometries of the films were obtained, which are presented from a smaller to a greater thickness: $BaTi(O_{0.16}S_{0.84})_3$, $BaTi(O_{0.26}S_{0.74})_3$, and $BaTi(O_{0.29}S_{0.71})_3$.

3.1.2. Crystal structure

Using the X-ray diffraction technique, it was possible to obtain the crystal structure of the precursor perovskite compound in powder form and of the thin films. Figure 1 shows the diffractograms belonging to both the precursor powder and the thin films of the $BaTi(O_{1-x}S_x)_3$ perovskite compound. The four diffractograms showed several peaks centered at 2 =21.57, 26.38, 30.88, 31.51, 34.35, 41.13, 43.89, 45.24 and 46.50, which are related to the (101), (110), (200), (002), (201), (210), (211), (202) and (300) planes, which belong to the hexagonal crystal structure of the $BaTiS_3$ perovskite [26–29]. Therefore, all thin films maintain the hexagonal crystalline structure, present in the perovskite precursor compound. As shown in the four diffractograms, for all samples there are three intense peaks; however, the most intense diffraction peak is related to the crystallographic plane (201). As can be observed, the intensity of the peaks in the diffractograms of the three thin films increased gradually for each of them, this effect is directly associated with the thickness

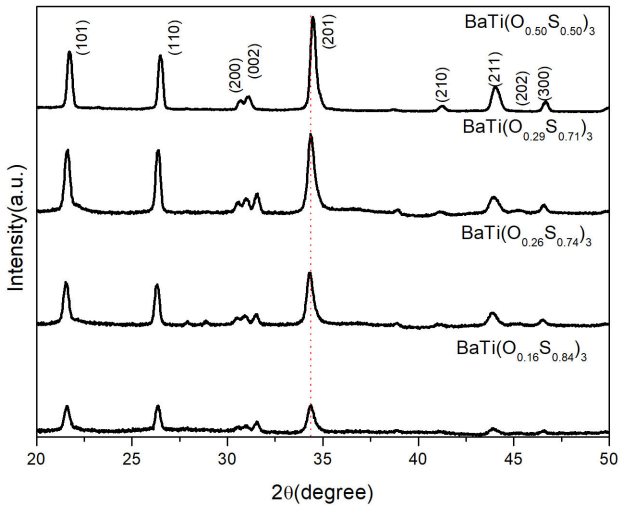

FIGURE 1. Diffractograms of the thin films and the precursor powder of the perovskites compound.

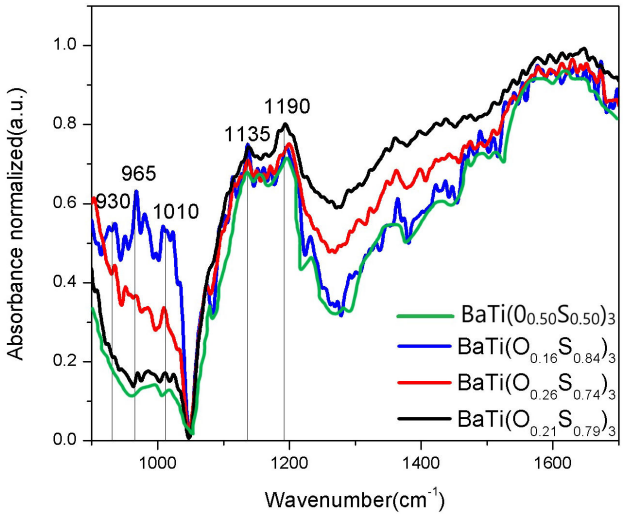

FIGURE 2. FTIR normalized absorption spectrum of precursor powder and the thin films of the perovskite compound BaTi($O_{1-x}S_x$)$_3$.

of the film; that is, the greater the thickness, the greater the intensity of the peaks. A slight shift to the right of the peaks in the diffractogram of the precursor powder can also be observed with respect to the diffractograms belonging to the thin films, which may indicate a larger crystal size in the perovskite powder compound.

To carry out a complete study of the crystalline structure of the precursor powder and the thin films of the perovskite compound BaTi($O_{1-x}S_x$)$_3$, the size of the crystals (D) was calculated using the Scherrer formula $D = (0.9)\lambda/\beta\cos\theta_\beta$, where λ is the wavelength of the X-rays used in diffraction (1.504 Å), β is the full width at half maximum (FWHM) of the main peak, and θ is the Bragg angle, the interplanar distances of the most intense peaks in the diffractograms from the equation of Bragg's law $d_{hkl} = \lambda/2\ \sin\theta_{hkl}$ where d is the interplanar distance and h, k and l are the Miller indices, and the lattice constants a and c correspond to the hexagonal crystalline structure. Crystallographic data obtained by Eq. (1) are shown in Table I:

$$\frac{1}{d_{hkl}^2} = \frac{4}{3}\frac{h^2+hk+k^2}{a^2} + \frac{l^2}{c^2}. \qquad (1)$$

As can be seen from the values obtained for the lattice constants, interplanar distances and grain size, for each of the films, no significant effects of the increase in sulfur are observed on the crystallographic parameters measured in each sample. As expected, the crystal size, interplanar distances and lattice constants of the precursor material are slightly larger. A possible explanation for this is the difference that exists in the materials when deposited in thin film and in bulk, but the most important thing is that the four diffractograms present the same peaks related to a hexagonal crystalline structure.

TABLE I. The diameters of the crystal, the full width at half maximum (FWHM) of the main peak, and the lattice constants, of the BaTi($O_{1-x}S_x$)$_3$ compounds.

Perovskite	D (Å)	$\beta_{(201)}$	a (Å)	c (Å)
BaTi($O_{0.50}S_{0.50}$)$_3$	240.82	0.5885	6.7212	5.7871
BaTi($O_{0.16}S_{0.84}$)$_3$	228.79	0.3548	6.5849	5.5334
BaTi($O_{0.26}S_{0.74}$)$_3$	225.86	0.3594	6.6050	5.5394
BaTi($O_{0.29}S_{0.71}$)$_3$	221.79	0.3660	6.5964	5.5314

3.2. Vibrational properties

The vibrational properties in the thin films were obtained from the FTIR spectroscopy technique. The absorption was measured in the range of 900 to 1700 cm^{-1}. The results are shown in Fig. 2.

The FTIR absorption spectra of the three perovskites showed several maximums at 930, 965, 1010, 1135, and 1190 cm^{-1}, the maximums centered at 930 and 965 cm^{-1} have been associated with the symmetric vibration band of SO_4^{-2}, the sulfur oxygen S-O bonds have been present in the region 1085-1179 cm^{-1}, and the C_2S=O bond is in the range 1150-1165 cm^{-1} [30–32]. It can be seen in the image that the spectrum associated with the BaTi($O_{0.16}S_{0.84}$)$_3$ film presents a greater definition in the maximums compared to the other two spectra associated with the two films; this behavior corresponds to the increase in the sulfur concentration and, at the same time, the substitution of oxygen by sulfur in the films, which provokes the formation of a greater number of bonds between sulfur and oxygen in the samples and therefore a higher intensity in the bands associated with these bonds.

3.3. Optical properties

3.3.1. *Normalized absorbance*

The absorption in the three samples of the perovskite compound BaTi($O-1-xS_x$)$_3$ was obtained from the Uv-Vis-

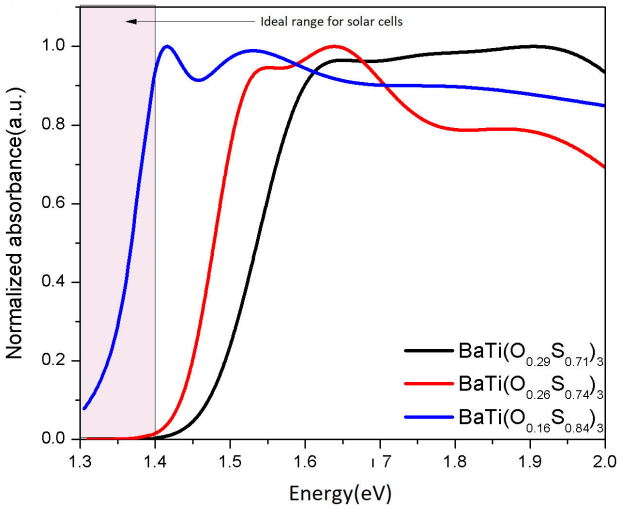

FIGURE 3. Normalized absorbance of the three $BaTi(O_{1-x}S_x)_3$ thin films.

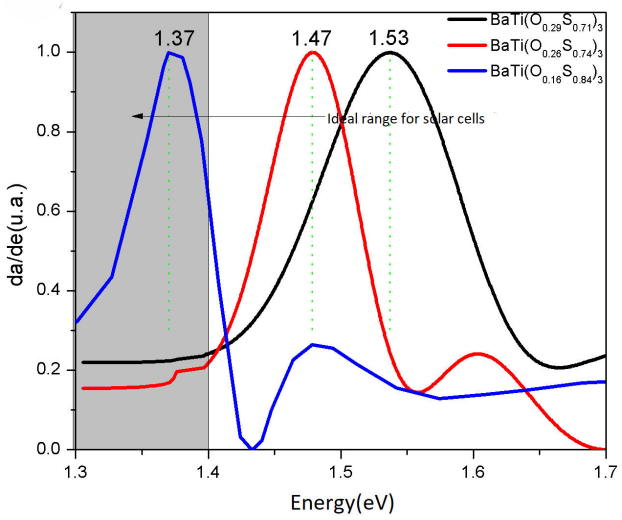

FIGURE 4. Derived from the normalized absorption of the three samples of the chalcogenide perovskite compound.

Nir spectroscopy technique in the range of 600 to 950 nm. The results obtained are shown in Fig. 3. The three samples have high absorption and show several absorption bands, those related to the forbidden bands of the films being those centered at 885, 818, and 750 nm for the $BaTi(O_{0.16}S_{0.84})_3$, $BaTi(O_{0.26}S_{0.74})_3$, and $BaTi(O_{0.29}S_{0.71})_3$ films respectively; a clear relationship can be seen between the mass percentage of sulfur shown in the thin films and a shift of the bands related to the forbidden band; the higher the percentage of S, the greater the band shift toward longer wavelengths.

A derivation was made to the absorption spectra with respect to the energy of the three thin films of the chalcogenide perovskite compound, the results are shown in Fig. 4. From the results it was possible to find the maximum absorption of each sample, this maximum can be related to the forbidden band width of each film, the results obtained were 1.37, 1.47 and 1.53 eV, for the perovskites $BaTi(O_{0.16}S_{0.84})_3$, $BaTi(O_{0.26}S_{0.74})_3$, and $BaTi(O_{0.29}S_{0.71})_3$, respectively. Among these results, the sample $BaTi(O_{0.16}S_{0.84})_3$ stands out because the width of its forbidden band is in the ideal region for its use as an active layer in a solar cell.

3.3.2. *Absorption coefficient and band gap*

The absorption coefficient present in the thin films of the perovskite compound $BaTi(O_{1-x}S_x)_3$ was obtained from the absorption spectrum measured in the range 600 to 950 nm and using the equation $\alpha = 2.303A/t$ derived from the Lambert-Beer law, where A is the absorption, t is the thickness of the film and α is the absorption coefficient. The absorption coefficients obtained are shown in Fig. 5.

The three thin films show a very high absorption coefficient [32], sample $BaTi(O_{0.16}S_{0.84})_3$ presents an absorption coefficient with a maximum of 5×10^4 cm^{-1} in the range of 600 to 883 nm, from here on there is an abrupt drop in absorption, the $BaTi(O_{0.26}S_{0.74})_3$ sample has a maximum in the absorption coeffcient of 4×10^4 cm^{-1} between 600 and 815 nm, after which it finds a considerable decrease in the absorption coefficient, and finally the $BaTi(O_{0.21}S_{0.79})_3$ film has an absorption coeffcient with a maximum of 4×10^4 cm^{-1} in the range of 600 to 775 nm; from this point, the absorption coeffcient drops abruptly. From these results, it can be seen that the three samples have a very high absorption coeffcient in all three cases with a maximum greater than 4×10^4 cm^{-1}, and as expected from what was observed in the absorbance curves, there is a direct relation between the sulfur percentage and the border of the absorption region in the films. According to the image shown in Fig. 3, the absorption range boundary is shifted to larger wavelengths directly proportional to the amount of sulfur in the sample, for a higher concentration of sulfur in the films, a broader absorption region was found.

The band gap that belongs to the three thin films of the perovskite compound $BaTi(O_{1-x}S_x)_3$ was calculated from

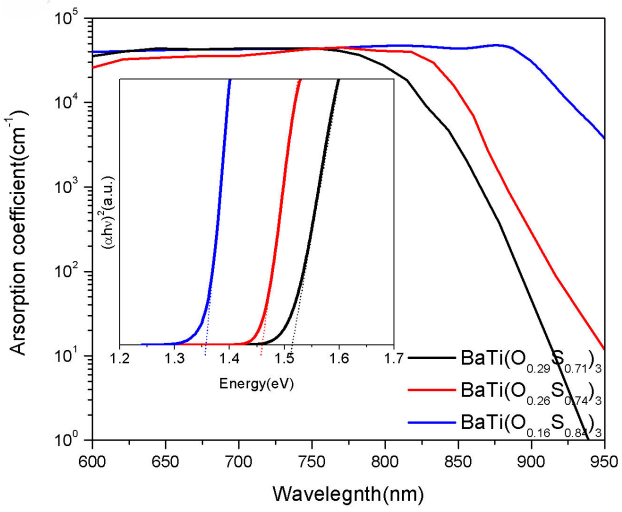

FIGURE 5. The absorption coefficient and the band gap of the three samples.

the Tauc method. The Tauc equation is defined as $\alpha h\nu = A(h\nu E_g)^n$ where alpha is the absorption coefficient, $h\nu$ is the photon energy and $n = 1/2$ that defines the type of transition as a direct allowed transition.

In the inset of Fig. 5 the values of the band gaps obtained from the three thin films are shown. The values obtained were 1.51 eV, 1.45 eV, and 1.35 eV for the samples BaTi($O_{0.29}S_{0.71}$)$_3$, BaTi($O_{0.26}S_{0.74}$)$_3$, and BaTi($O_{0.16}S_{0.84}$)$_3$, respectively. Two interesting properties can be highlighted from these results; the first is the direct dependence that exists between the concentration of sulfur in the samples and the band gap width. The band gap of BaTi($O_{1-x}S_x$)$_3$ can be adjusted using sulfur concentration as a control, with a higher percentage of sulfur, a smaller width in the band gap. The second important result is that the band gap values are within the ideal range of the widths for the band gap of active materials used in solar cells, which is 1.4 to 1.1 eV [15], so the three films and specifically the sample BaTi($O_{0.16}S_{0.84}$)$_3$ has the characteristics for its application in solar cells.

4. Discussion

A considerable increase in the presence of sulfur is observed in the three thin films after being subjected to heat treatment in a CS_2 atmosphere, the increase in the sulfur concentration and the consequent reduction of oxygen in the sample were proportional to the thickness of the thin films. The film with a lower amount of material had a greater increase in the percentage of sulfur; this can be explained by the Gibbs-Duheim relation [33] given in Eq. (2). This expression says that when the temperature and pressure are constant, the chemical activation potential is proportional to the amount of annealed material.

$$\sum_{i=1}^{I} N_i d\mu_i = -SdT + VdP, \tag{2}$$

where N is the number of particles, μ the chemical potential, S the entropy, T the temperature, V the volume, and P the pressure. Since all the heat treatments given to the thin films were carried out at a constant temperature and pressure, we are left with:

$$d\mu = \frac{1}{N}, \tag{3}$$

the chemical activation potential is inversely proportional to the amount of annealed material. Therefore, it can be stated that the chemical potential is the cause of the exchange of S for O.

The hexagonal crystalline structure typical of the $BaTiS_3$ chalcogenide perovskite and present in the BaTi($O_{0.5}S_{0.5}$)$_3$ used as the precursor, was maintained in the thin films deposited and annealed. All of the thin films show excellent crystallinity, with similar sizes of crystallite, and practically without changes in the lattice parameters, according to the results obtained.

Furthermore, in direct correlation with the increase in the percentage of sulfur, the vibrational modes observed in the three films show larger intensity signals for the bands related to sulfur-oxygen bonds. The film with a greater amount of sulfur shows more defined bonds and confirms the formation of a quaternary material, as previously reported in recent publications [36], resulting in the formation of oxysulfide as an anion in the chalcogenide perovskite compound.

Finally, the most novel result of this work was found in the optical properties of the BaTi($O_{1-x}S_x$)$_3$ perovskite thin films; they have a very high absorption coefficient greater than 5×10^4 cm^{-1} and band gap values in the range of 1.6 and 1.35 eV, which are within the ideal range required for active materials in the application of solar cells. With this value in the band gap of BaTi($O_{1-x}S_x$)$_3$ perovskite thin films, it is also demonstrated that chalcogenide perovskites can reach band gap values between 1.3 and 1.4 eV, as has been theoretically proposed and a situation that until now has been very difficult to achieve in practice using only sulfur or selenium in the anion site. The band gap of the perovskite films is closely linked to the amount of sulfur and oxygen in thin films, and this behavior is explained by the differences in the electronic configuration that exist between oxygen and sulfur, since the surplus orbitals present in sulfur 3s and 3p generate a large number of states in the valence band, which reduces the width of the band gap. It is important to note that the reduction in the band gap occurs in a gradual form using the sulfur and oxygen concentrations as a control, and the hexagonal crystalline structure of the perovskite remains for all the samples [34, 35, 37].

5. Conclusions

Thin films of the oxysulfide perovskite compound were deposited using the spin-coating deposition technique. All films presented the hexagonal crystalline structure of the perovskite and very advantageous optical characteristics for their possible application in solar cells, the most important optical property being a tunable band gap depending on the percentage of sulfur incorporated into the sample, which has been shown to reach values close to the ideal value of 1.3 eV. The sample BaTi($O_{0.16}S_{0.84}$)$_3$, with a thickness of 289 nm, is the one that stands out the most in this sense, showing an absorption coefficient greater than 4×10^4 cm^{-1} in the range of 600 to 883 nm and a band gap of 1.35 eV, which are ideal properties for perovskites used as active layer in solar cell structures. Finally, based on these results, we propose the fabrication of a p-i-n type solar cell structure, using spiro-MeOTAD, the perovskite compound in the intrinsic layer, as the p-type conductor and TiO_2 as the n-type semiconductor.

1. K. V. Sopiha, C. Comparotto, J. A. Mrquez, J. J. S. Scragg, Chalcogenide Perovskites: Tantalizing Prospects, Challenging Materials, *Advanced Optical Materials* **10** (2022). https://doi.org/10.1002/adom.202101704
2. S. Abhishek, J. M.Wasim, C. Rayan, J. Metikoti, S. Tariq, N. Angshuman, Are Chalcogenide Perovskites an Emerging Class of Semiconductors for Optoelectronic Properties and Solar Cell?. *Chemistry of Materials* **31** (2019) 565-575. https://doi.org/10.1021/acs.chemmater.8b04178.
3. S. Dahbi, N. Tahiri, O. El Bounagui, H. Ez-Zahraouy, The new ecofriendly lead-free zirconate perovskites doped with chalcogens for solar cells: Ab initio calculations, *Optical Materials* **109** (2020) 110442, https://doi.org/10.1016/j.optmat.2020.110442.
4. D. Tiwari, O. S. Hutter, and G. Longo, Chalcogenide perovskites for photovoltaics: current status and prospects, *J. Phys. Energy* **3** (2021) 034010, https://doi.org/10.1088/2515-7655/abf41c.
5. S. J. Adjogri, and E. L. Meyer, Chalcogenide Perovskites and Perovskite-Based Chalcohalide as Photoabsorbers: A Study of Their Properties, and Potential Photovoltaic Applications, *Materials* **14** (2021) 7857; https://doi.org/10.3390/ma14247857.
6. S. Perera *et al*., Chalcogenide perovskites an emerging class of ionic semiconductors, Nano Energy, **22** (2016) 129-135,
7. M. Buffiere, D.S. Dhawale, F. El-Mellouhi, Chalcogenide Materials and Derivates for Photovoltaic Applications, *Energy Technology* (2019) https://doi.org/10.1002/ente.201900819.
8. V.K. Ravi, S.H. Yu, P.K. Rajput, C. Nayak, D. Bhattacharyya, D.S. Chung, A. Nag, Colloidal BaZrS3 Chalcogenide Perovskite Nanocrystals for Thin Film Device Fabrication, *Nanoscale*, (2021) https://doi.org/10.1039/D0NR08078K.
9. M. Ju, J. Dai, L. Ma, and X. C. Zeng. Perovskite Chalcogenides with Optimal Bandgap and Desired Optical Absorption for Photovoltaic Devices, *Adv. Energy Mater.* (2017) 1700216. https://doi.org/10.1002/aenm.201700216.
10. H.I. Eya, E. Ntsoenzok, N.Y. Dzade, First principles Investigation of the Structural, Electronic, and Optical Properties of - and -SrZrS3: *Implications for Photovoltaic Applications*, *Materials* (2020), https://doi.org/10.3390/ma13040978.
11. W. Shockley and H.J. Queisser, Detailed Balance Limit of Efficiency of p-n Junction Solar Cells, *Journal of Applied Physics*, **32** (1961) 510-519; https://doi.org/10.1063/1.1736034.
12. S. ruhle, Tabulated vakues of the Shockley-Queisser limit for single junction solar cell, *Solar Energy*, **130** (2016) 139-147; https://doi.org/10.1016/j.solener.2016.02.015.
13. T.A. Bhere *et al*., Organometal Halide Perovskite Solar Cells: Degradation and Stability. *Energy Environ. Sci*., **9** (2016) 323356, https://doi.org/10.1039/C5EE02733K.
14. C. Comparotto *et al* The Chalcogenide perovskite BaZrS3: Thin film growth by sputtering and rapid thermal processing, *Energy Materials*, (2020). https://doi.org/10.1021/acsaem.9b02428.
15. S. Niu *et al*., Bandgap Control via Structural and Chemical Tuning of Transition Metal Perovskite Chalcogenides, *Adv. Mater*. (017) 1604733. https://doi.org/10.1002/adma.201604733.
16. H. Chen *et al.*, Molten flux growth of single crystals of quasi-1D hexagonal chalcogenide BaTiS3. *Journal of Materials Research* **39** (2024) 1901-910, https://doi.org/10.1557/s43578-024-01379-5.
17. S. V. Mauritz *et al.*, Precursor Selection Strategies for Two-Dimensional Anisotropic Growth and Morphological Control of BaTiS3 *Nanocrystals*. *Chemistry of Materials*, **37** (2025) 6552-6561 https://doi.org/10.1021/acs.chemmater.5c00956.
18. M. Surendran *et al*., Quasi-epitaxial growth of BaTiS3 films. *Journal of Materials Research* **37** (2022) 3481-3490. https://doi.org/10.1557/s43578-022-00776-y.
19. L. C. Fu,W. J. Cheng,Y. Liu,L. C. Shi,Y. Peng,J. Zhang,Z. W. Li,X. D. Li,J. L. Zhu,X. C. Wang and C. Q. Jin. Structure and properties of a quasi-one-dimensional compound BaTiS3 under pressure, *High Pressure Research*, Pages 95-104, 2024 https://doi.org/10.1080/08957959.2024.2325994
20. C. Chaomin, L. Ruiming, S. Zhang, R. He, Y. Sun, M. Yang, Y. Liu, H. Liu, Preparation of BaTiS3 film under lower temperature and its Application in Photodetectors, *Thin Solid Films*, **835** (2026) 140858, https://doi.org/10.1016/j.tsf.2026.140858.
21. T. Le Bahers, M. Rerat, and P. Sautet. Semiconductors Used in Photovoltaic and Photocatalytic Devices: Assessing Fundamental Properties from DFT. *The Journal of Physical Chemistry C* **118** (2014) 5997-6008. https://doi.org/10.1021/jp409724c.
22. J. Liu, S. Zhang, M. Jiang, H. Xiao, S. Feng, L. Qiao, Electronic structure and anion engineering for perovskite oxysulfide BaTi(O, S)3. *J Vacuum Sci Technol*, **40** (2022) 012801. https://doi.org/10.1116/6.0001471
23. N. Vonruti, U. Aschauer, Band-gap engieneering in AB(OxS1-x)3 perovskite oxisulfides: a route to strongly polar materials for photocatalytic water splitting. *J Mater Chem A* 7 (26), https://doi.org/10.1039/.2019:1574115748.
24. U. Ahmed, M. M. Hossian, M. M. Uddin, N. Jahan, and M. A. Ali, Tuning the opto-electronic properties of BaTiO3 by S substitution towards energy harvesting applications: a DFT insight using the VASP code, *Mater. Adv.*, **7** (2026) 403-424, https://doi.org/10.1039/D5MA00882D.
25. R. Gomez-Rosales *et al*., Bandgap engineering of BaTi(O1-xSx)3 as a function of sulfur concentration, *J Mater Sci*, Issue 21/2023. https://doi.org/10.1007/s10853-023-08586-1.
26. B. Kai, K. Takahashi, M. Saeki, J. Yoshimoto, Preparation and crystal structures of some complex sulphides at high pressures. *Mater Res Bull* **23** (1988) 15751584, https://doi.org/10.1016/0025-5408(88)90245-0.
27. S. Wang *et al*., Phasedependent band gap engineering in alloys of metal-semiconductor transition metal dichalcogenides. *Adv Funct Mater*, (2020). https://doi.org/10.1002/adfm.202004912.

28. K. Tewatia, A. Sharma, M. Sharma, A. Kumar, Factors affecting morphological and electrical properties of Barium Titanate: a brief review. *Mater Today* **44** (2020) 454856,

29. Y. Morino, T. Masahara, K. Itoh, The synthesis and crystal structures of some alkaline earth Titanium and Zirconium Sulfides. *Acta Cryst* **16** (1963) 135142,.

30. H. Hahn, U. Mutschke. Untersuchungen uber tern are Chalkogenide. XI. Versuche zur Darstellung von Thioperowskiten. *J Inorg Gen Chem* **288** (1957) 269278 https://doi.org/10.1002/zaac.19572880505.

31. D, Zilevu, S. Creutz. Shape-controlled synthesis of colloidal nanorods and nanoparticles of Barium Titanate Sulfide. *Chem Mater* **33** (2021) 51375146

32. Y. Sun, F. Zhang, D. Wu, H, Zhu, Roles of polyacrylate dispersant in the synthesis of well-dispersed BaSO4 nanoparticles by simple precipitation. *Particuology*, (2013). https://doi.org/10.1016j.partic.2013.02.005.

33. R. A. Alberty. Use of Legendre transforms in chemical thermodynamics (PDF). *Pure Appl. Chem.* **73** (2021) 1349-1380, https://doi.org/10.1351/pac200173081349.

34. R. Fang, W. Zhang, S. Zhang , W. Chen, The rising star in photovoltaics-perovskite solar cells: the past, present and future. *Sci China Tech Sci*, (2016). https://doi.org/10.1007/s11431-016-6056-8

35. T. Le Bahers, M. Rerat, P. Sautet,Semiconductors used in photovoltaic and photocatalytic devices: assessing fundamental properties from DFT. *J Phys Chem C* **118** (2014) 59976008. https://doi.org/10.1021/jp409724c.

36. J. Liu, S. Zhang, M. Jiang, H. Xiao, S. Feng, L. Qiao, Electronic structure and anion engineering for perovskite oxysulfide BaTi(O, S)3. *J Vacuum Sci Technol A* **40** (2022) 012801, https://doi.org/10.1116/6.0001471 8.

37. E. Abdul and R. Assirey, Perovskite synthesis, properties and their related biochemical and industrial application, *Saudi Pharmaceutical Journal*, **27** (2019) 817829, https://doi.org/10.1016/j.jsps2019.05.003.